Polymer 50 (2009) 966–972

Contents lists available at ScienceDirect

Polymer

journal homepage: www.elsevier.com/locate/polymer

Synthesis and self-assembly in bulk of six-arm star-block copolymers with a C_{60} core

Bruno Schmaltz, Claude Mathis, Martin Brinkmann*

Institut Charles Sadron, CNRS-ULP, 23 rue du Loess, BP 84047, 67034 Strasbourg Cedex 2, France

ARTICLE INFO

Article history:
Received 14 November 2008
Accepted 18 December 2008
Available online 25 December 2008

Keywords:
Self-assembled structures
Star-block copolymers
Fullerenes

ABSTRACT

This study focuses on the synthesis and the structural characterization of various branched star-block copolymers (polyisoprene-*block*-polystyrene)$_6$C$_{60}$ with a fullerene C_{60} as a core. Well defined 6-arm stars (PI-*b*-PS)$_6$C$_{60}$ with a low polydispersity and a precise control of the number of branches were prepared by grafting PI-*b*-PS diblock copolymers through the polystyrene block onto the C_{60} core. The self-assembled structures formed in bulk were studied by Transmission Electron Microscopy (TEM) and Small Angle X-ray Scattering (SAXS) for both symmetric and asymmetric polystyrene-*block*-polyisoprene (PS-*b*-PI) diblock arms in the strong-segregation regime ($65 \le \chi N \le 115$). Various microstructures including lamellae, hexagonal packings of PS and PI cylinders as well as a gyroid phase were obtained by varying the volume fraction of polystyrene (f_{PS}) of the branches, leading to the formation of ordered, periodic and localized nanoscale dispersions of the C_{60} in a polymer matrix including planes, threads and a 3D bicontinuous network of C_{60}.

1. Introduction

Block copolymers are widely used for the fabrication of nanomaterials because of their intrinsic ability to self-assemble into well-ordered and periodic microstructures (lamellae, cylinders, bicontinuous gyroid, spheres) with characteristic dimensions in the submicrometer range [1–4]. These microstructures have been successfully employed as a structuring matrix for the controlled nanoscale dispersion of different nano-objects e.g. Pd, SiO_2 and Au nanoparticles [5–7], providing potentially new and original materials with unique optical, electronic or magnetic properties at the nanoscale. Precise location of nano-objects in the copolymer matrix can be achieved via proper surface functionalization of the nanoparticles so as to ensure compatibility with one of the block domains [7]. The controlled dispersion of molecular species like C_{60} in a copolymer matrix is a rather difficult task due to its low solubility and intrinsic tendency to aggregate. Grafting polymer [8,9] or copolymer chains [10] on C_{60} constitutes an elegant and efficient way to overcome the solubility limit of C_{60} in organic solvents and to achieve a homogeneous dispersion of C_{60} in a polymer matrix. In a previous study, we have demonstrated that star-shaped macromolecules with a C_{60} core can be dispersed in a controlled way in the lamellar microstructure of a diblock copolymer [11]. This method leads to an ordered and periodic spatial dispersion of the C_{60} in the polymer matrix by selective solubilization of the homopolystyrene stars e.g. (PS)$_6$C$_{60}$ into the PS domains of a polystyrene-*b*-polyisoprene (PS-*b*-PI) diblock copolymer. Different regimes of solubilization of (PS)$_6$C$_{60}$ stars in the lamellar structure of the copolymer were identified. However, this solubilization depends on the total load of stars in the copolymer and also on the size of the stars with respect to the lamellar periodicity. An alternative way to reach a self-separated microstructure with a well defined nanoscale dispersion of the C_{60} consists in grafting directly the self-assembling diblock copolymer on the C_{60} core to obtain star-block copolymers e.g. (PI-*b*-PS)$_6$C$_{60}$.

In the present communication, we will first describe the synthesis of the copolymer stars and then discuss the structure of the self-assembled stars in the bulk which have been identified by using Transmission Electron Microscopy and Small Angle X-ray Scattering (SAXS). We will show that self-assembly of copolymer stars (PI-*b*-PS)$_n$C$_{60}$ with $n = 6$, in bulk, allows to obtain several microstructures (lamellae, hexagonal packing of cylinders and gyroid) by varying the relative length of the PS and the PI blocks. In particular, we demonstrate the possibility to obtain a gyroid phase in which the cores of the stars, i.e. the C_{60}s, are exclusively confined to the minority phase domains of PS forming two 3D bicontinuous interpenetrated networks in the PI matrix.

---

* Corresponding author. Tel.: +33 3 88 41 40 47; fax: +33 3 88 41 40 99.
E-mail address: brinkman@ics.u-strasbg.fr (M. Brinkmann).

0032-3861/$ – see front matter © 2008 Elsevier Ltd. All rights reserved.
doi:10.1016/j.polymer.2008.12.034

2. Experimental section

2.1. Materials

Toluene free of protonic impurities was distilled directly into the glass apparatus from a red solution of 3-methyl-1,1-diphenylpentyllithium. Styrene and isoprene (Aldrich), distilled first over sodium, were further distilled in ampoules equipped with break-seals from an *n*-butyllithium solution (prepolymerization). To remove impurities present in commercial fullerene, C_{60} (>99% from SES Research) was stirred several hours in pure THF and recovered by centrifugation. This procedure was repeated until a colorless THF solution was obtained. The C_{60} was then dried under high vacuum ($<10^{-5}$ Torr) at 100–150 °C, kept and handled under argon in a glovebox. *sec*-Butyllithium (*s*-BuLi) was prepared by reacting 2-chlorobutane with lithium metal in cyclohexane and its concentration determined by titration.

2.2. Synthesis of the (PI-b-PS)$_6$C$_{60}$ stars

The synthesis was performed in a glass apparatus sealed under high vacuum (10^{-5} Torr) using the break-seal technique [8,12]. The polyisoprene-*b*-polystyrene diblock copolymers (PI-*b*-PS) were prepared in toluene using *sec*-butyllithium (*s*-BuLi) as the initiator. For various reasons discussed latter (see Section 3.1), the polyisoprene block was prepared first. The polymerization of isoprene was conducted at room temperature for 3 h and then heated to about 40 °C for three additional hours to ensure complete conversion. After removing an aliquot for characterization, styrene was added slowly by internal distillation over about one hour and, once all the monomer was introduced, the polymerization was allowed to continue for 3 h at room temperature. C_{60} was subsequently added in a 1:8 ratio vs. the initial concentration of s-BuLi and the addition reaction allowed to run over night at room temperature. Finally, a small quantity of degazed methanol containing a few % of HCl was added, the sealed apparatus was opened and the polymer was recovered by precipitation in methanol. The (PI-*b*-PS)$_6$C$_{60}$ stars were separated from the ungrafted PI-*b*-PS chains by polymer fractionation. This was achieved in a classical fractionation setup by adding methanol to a stirred toluene solution of the crude product (about 1 g/l) at room temperature until the solution became cloudy. The solution was then heated until it became again completely transparent and then cooled very slowly to room temperature (over about two days) allowing the (PI-*b*-PS)$_6$C$_{60}$ stars to be separated from the excess of PI-*b*-PS branches.

2.3. Characterization

The various samples were characterized by multiple detector Size Exclusion Chromatography (SEC) using THF as the eluent and a PS calibration. The SEC setup consisted of a Shimadzu LC10AD pump, an ERMA ERC3512 on-line degasser, a WATERS automatic injector and five 300 × 7.5 mm PL Gel columns from Polymer Laboratories (4 × 10 μm Mixed-B and one 500 Å) connected in series and a refractive index (RI) detector (Shimadzu RID10A). To determine the actual molar mass of the star-shaped polymers, an on-line Light Scattering (LS) detector (MALLS DAWN DSP from Wyatt Technology) was also used. As 100% of the monomers were polymerized and no deactivation of the carbanions was detected (no PI chains present in the SEC analysis of the final product), the d*n*/d*c* used for the copolymers was calculated from the amounts of isoprene and styrene used in the synthesis.

2.4. Sample preparation for TEM and SAXS analysis

Bulk samples of (PI-*b*-PS)$_6$C$_{60}$ stars were prepared by casting from toluene solutions (concentration of 5 wt%), a nonselective solvent for polystyrene and polyisoprene. In order to avoid sample's oxidation during slow evaporation of toluene, 0.5 wt% of an anti-oxidant agent (Vukanox KB) was added to the solutions. The samples were left for slow solvent evaporation over 14–21 days in ambient and sheltered from light and subsequently dried under primary vacuum (10^{-3} mbar) for 3–4 days. Samples were prepared in the form of discs with a diameter of 1 cm and a thickness of 1–2 mm. The volume fractions of PS were calculated by using the following densities of PS and PI at room temperature: 1.03 and 0.86 g/cm^3.

2.5. Transmission electron microscopy

For TEM characterization, bulk samples were microtomed at low temperature (approximately −80 °C) using a Leica Ultracut S microtome with a FCS cryo temperature attachment. The sections of nominal thickness 50–70 nm were stained with OsO_4 vapors. The sections were examined in bright-field mode using a Philips CM 12 transmission electron microscope at 120 kV and a MVIII camera (Soft Imaging Systems). In all TEM micrographs, the dark regions correspond to osmium-stained polyisoprene domains.

2.6. Small angle X-ray scattering

The structure of the samples was further investigated by using small-angle X-ray scattering (SAXS) on a Bruker diffractometer equipped with a copper anode (Cu Kα, $\lambda = 0.1542$ nm) at an accelerating voltage of 40 kV and a filament current of 40 mA. The scattered intensities were collected on a Highstar (Bruker) two-dimensional position-sensitive detector placed ∼1 m from the sample and were corrected for wire sensitivity, parasitic scattering and geometric parameters. The angular calibration of the SAXS system was accomplished with a silver behenate sample.

3. Results and discussion

3.1. Synthesis and characterization of the (PI-b-PS)$_6$C$_{60}$ stars

It has been demonstrated that the terminal polystyryl or polyisoprenyl carbanions of PSLi, PILi or PS-*b*-PILi can add to the C_{60} by opening a 6-6 "double" bond on the fullerene [8,10]. However, this reaction has to be conducted in a non-polar solvent as the presence of even small amounts of a polar solvent favors electron transfer from the carbanion to the fullerene over the addition of chains [8]. Toluene was chosen since it is one of the best solvents for C_{60} and because, even if proton abstraction from toluene by the carbanions can take place, this side reaction is slow enough to be neglected during the time needed for polymerization or addition to the fullerene. It has also to be noted that the grafting of PILi or PS-*b*-PILi onto C_{60} leads to the formation of a rather weak PI-fullerene bond and the resulting stars are unstable even at room temperature [10]. This observation results from the presence of a double bond in the vicinity of the C_{60}-PI link leading to breaking through a 1,5-sigmatropic H-shift [10]. This is not the case if a PS chain is linked to the fullerene so that the PS-C_{60} bond is stable for years at room temperature although the thermal stability of $(PS)_xC_{60}$ stars is somewhat reduced as compared to PS because, as shown in previous studies, the PS-C_{60} link is easier to break than a C–C bond in the PS chain [13–15]. In addition, as demonstrated in previous studies [8–10], a maximum of 6 chains can be grafted onto the C_{60} using PS^-Li^+ in excess of 6 per fullerene leading to large amounts of perfectly defined 6-arm stars $(PS)_6C_{60}$ [16]. Since PI-*b*-PS^-Li^+ and PS^-Li^+ bear the same terminal carbanion, their reactivity toward C_{60} is identical and a 6-arm star $(PI\text{-}b\text{-}PS)_6C_{60}$ is obtained upon reacting the fullerene with an excess of the "living" copolymer. The synthetic method of the 6-arm stars $(PI\text{-}b\text{-}PS)_6C_{60}$ used in the present work is illustrated in Fig. 1. The first step in the preparation of the stars was to synthesize tailored "living" copolymers of PI-*b*-PS^-Li^+ using anionic polymerization. The initiation of the polymerization of styrene by PILi being known to be somewhat slower than that of isoprene by PSLi, a small amount of THF is generally added to PILi before addition of styrene to get PI-*b*-PS block copolymers with narrow polydispersities. This procedure could not be followed in the present case since the addition of PI-*b*-PSLi onto C_{60} requires the use of a completely non-polar medium. A slow addition of styrene to PILi allowed producing block copolymers of narrow polydispersity in pure toluene as shown by the SEC characterization reported in Table 1. In addition, the absence of any unreacted PI in the SEC traces of the products (Fig. 2) demonstrates that all the PILi have initiated styrene. PI-*b*-PSLi was further reacted in a large excess (>6:1) with C_{60} in order to produce the desired 6-arm star $(PI\text{-}b\text{-}PS)_6C_{60}$. The excess of ungrafted PI-*b*-PS chains is removed by classical polymer fractionation to obtain the pure 6-arm stars. As an example, the SEC traces for the PI block, the copolymer PI-*b*-PS and the star are shown in Fig. 2 ($f_{PS} = 0.77$). Beside molar masses of the polymers used in this study, Table 1 includes the experimental functionality of the stars determined by dividing the molar mass of the star by that of the copolymer determined by Light Scattering (LS) as well as the volume fraction of PS in the copolymer stars. All the 6-arm stars used in this study have been labelled $ST_6\text{-}M_w^{PS}\text{-}M_w^{PI}$ where M_w^{PS} and M_w^{PI} are the molecular masses of the PS and the PI blocks (expressed in kg/mol).

Table 1
Characteristics of the 6-arm star-block copolymers as obtained by Size Exclusion Chromatography (SEC) using PS calibration and by Light Scattering (LS).

Samples		SEC (RI)		LS	Functionality	f_{PS}
		$M_w \times 10^3$	M_w/M_n	$M_w \times 10^3$		
ST_6 8-27	PI block	41,4	1,07	27	6,2	0,20
	PI-*b*-PS	48,9	1,10	35		
	$(PI\text{-}b\text{-}PS)_6C_{60}$	222	1,14	220		
ST_6 11-34	PI block	52,4	1,05	34	6,1	0,22
	PI-*b*-PS	66,4	1,07	45		
	$(PI\text{-}b\text{-}PS)_6C_{60}$	273	1,09	277		
ST_6 12-21	PI block	31,8	1,07	21	5,8	0,33
	PI-*b*-PS	45,0	1,10	33		
	$(PI\text{-}b\text{-}PS)_6C_{60}$	176	1,06	192		
ST_6 25-15	PI block	22,4	1,08	15	5,8	0,59
	PI-*b*-PS	48,9	1,05	40		
	$(PI\text{-}b\text{-}PS)_6C_{60}$	204	1,09	230		
ST_6 25-25	PI block	40,0	1,06	25	6,0	0,46
	PI-*b*-PS	65,0	1,07	50,0		
	$(PI\text{-}b\text{-}PS)_6C_{60}$	283	1,11	300		
ST_6 56-14	PI block	21,3	1,08	14	6,0	0,77
	PI-*b*-PS	80,1	1,06	70		
	$(PI\text{-}b\text{-}PS)_6C_{60}$	344	1,13	420		

3.2. Morphology of microphase separated bulk samples

3.2.1. Lamellar and cylinder morphologies

Fig. 3 depicts the characteristic SAXS pattern obtained for a bulk sample of an ST_6-25-25 sample having symmetric PS-*b*-PI diblock arms. As expected for a symmetric copolymer [17], the SAXS pattern is characteristic of a lamellar microstructure and shows three peaks at q*, 2q* and 3q*. The lamellar periodicity extracted from the SAXS trace amounts to ca. 35 nm. This lamellar microstructure is also clearly evidenced by TEM (see inset in Fig. 3). Note the typical grain boundary of a lamellar structure in the bottom left corner of the inset which consists of a succession of edge dislocations. Due to the star-shape architecture of the copolymer, the C_{60} core is located close to the center of the PS lamellae. Assuming that all C_{60}s lie within a plane at the center of the PS lamellae [18], we can estimate the average inter-C_{60} distance to ~8 nm. The actual $C_{60}\cdots C_{60}$ distances are somewhat larger as statistical fluctuations of the fullerenes around these "ideal" positions are expected. Clearly, this distance is too large to allow any efficient charge transport by hopping but it might be decreased significantly by lowering the size of the PS-*b*-PI arms grafted on the C_{60} core. The lamellar structure is maintained by increasing or decreasing the volume fraction of PS within a given range. For instance, a star-block copolymer with dissymmetric branches e.g.

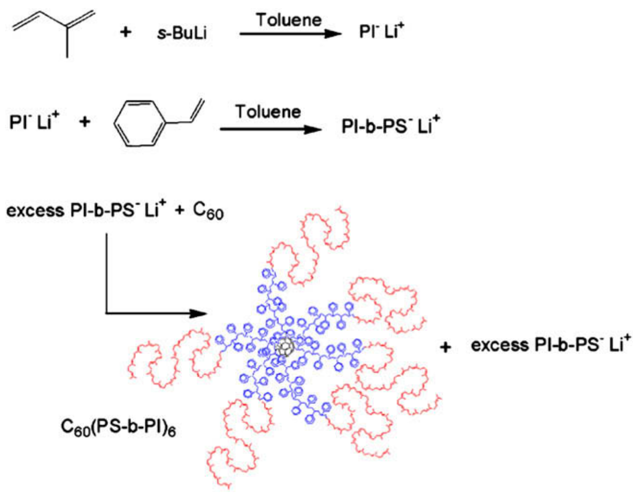

Fig. 1. Scheme of the synthetic route used to prepare the 6-arm star-block copolymers with a C_{60} core.

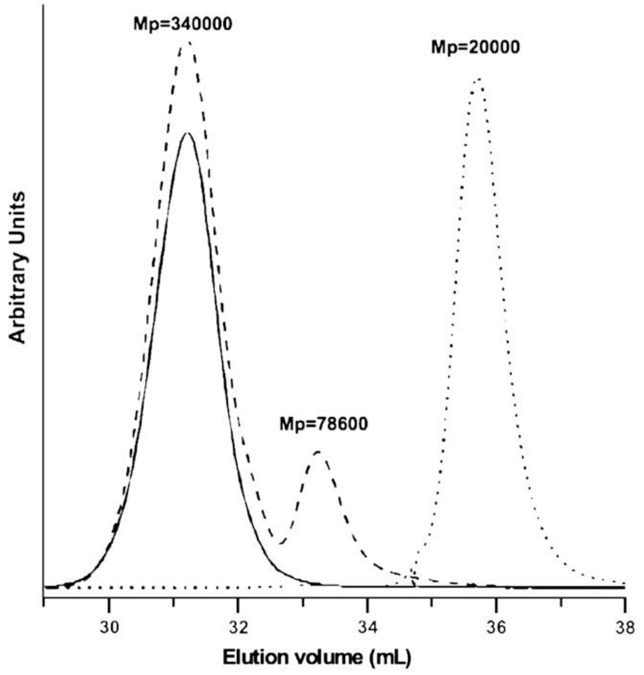

Fig. 2. SEC traces (RI detector – PS calibration) of the polyisoprene block ($M_p = 20.0$ kg/mol, dotted line), the crude addition product of block copolymer PI-*b*-PS ($M_p = 78.6$ kg/mol) onto C_{60} (8 PI-*b*-PS/C_{60}, dashed line) and the copolymer star $(PI\text{-}b\text{-}PS)_6C_{60}$ after fractionation (solid line) for the sample $ST_6$56-14 (see Table 1). M_p corresponds to the molar mass at the maximum of the peak.

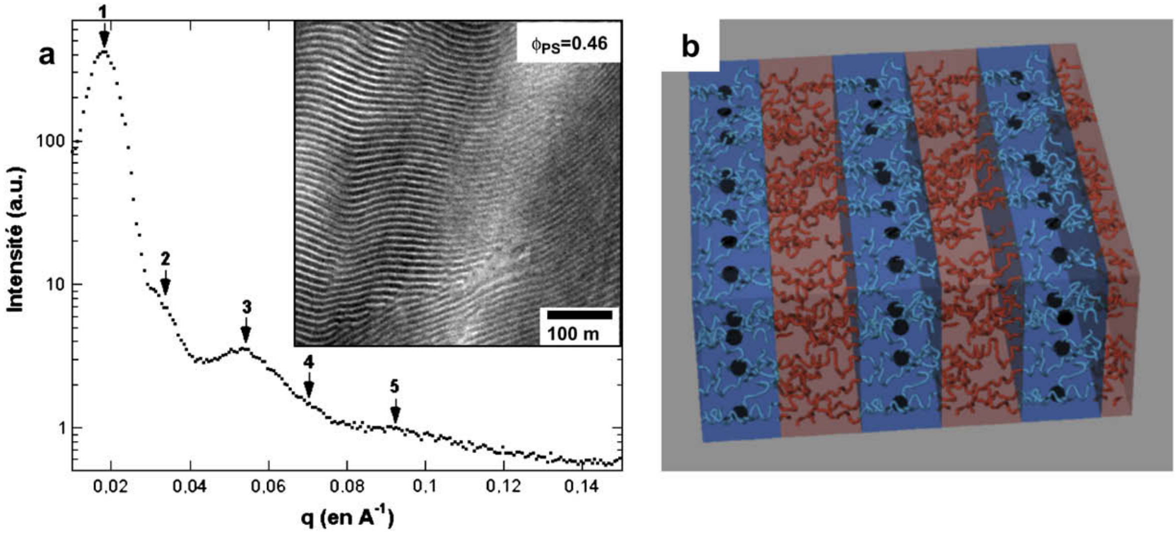

Fig. 3. a) SAXS trace of a bulk sample of ST$_6$-25-25. The inset corresponds to the TEM BF image showing the lamellar morphology. OsO$_4$-stained PI lamellae appear dark grey. b) Schematic illustration of the organization of the block copolymer stars in a lamellar morphology. The PI domains are represented in red, PS domains in blue and the C$_{60}$ as black spheres. (For interpretation of the references to color in this figure legend, the reader is referred to the web version of this article.)

ST$_6$25-15 still shows a lamellar microstructure with a periodicity of 24 nm.

By grafting asymmetric PS-*b*-PI arms on the C$_{60}$ core, we also obtained various cylinder morphologies. In Fig. 4a, we depict the SAXS pattern and the TEM BF of a bulk sample of ST$_6$-11-34 corresponding to a volume fraction of polystyrene of 0.22. The SAXS pattern shows a set of three well defined peaks located at q^*, $\sqrt{3}q^*$ and $\sqrt{7}q^*$ characteristic of the cylinder phase and the hexagonal packing of PS cylinders in a PI matrix is clearly observed in the inset of Fig. 4a corresponding to the TEM BF image. The periodicity deduced from the SAXS amounts to 30 nm for ST$_6$-11-34. This periodicity can be changed by controlling the average molecular weight of the PS-*b*-PI arms. A cylinder phase with $f_{PS} = 0.20$ and a periodicity of 23 nm was observed for ST$_6$-8-27. As for the lamellar phase, the ordered domains are observed to extend over several microns. Peculiar to this cylinder phase is the fact that the cores of the stars i.e. the C$_{60}$s are confined to the PS cylinders leading to the formation of C$_{60}$ "threads" as illustrated in Fig. 4b.

By increasing the volume fraction of PS to 0.77, we have obtained a cylinder phase consisting of a hexagonal packing of PI cylinders in a PS matrix (Fig. 5a). In this microstructure, the C$_{60}$ cores of the stars are located exclusively on the outside of the PI cylinders as shown in the schematic illustration of Fig. 5b leading to a homogeneous dispersion of C$_{60}$ in the PS matrix.

Therefore, depending on the volume fraction of the PS inner block of the (PI-*b*-PS)$_6$C$_{60}$ star-block copolymers, the C$_{60}$s can be either confined to or excluded from the cylinders of the minority phase.

3.2.2. Gyroid structure

In Fig. 6, we depict representative morphologies observed on ~50 nm-thick sections obtained by cryo-microtoming bulk ST$_6$12-21 samples. Highly ordered domains with uniform orientation are found to extend over several microns. The periodic patterns observed by TEM are clearly distinct from the projections expected for microstructures like lamellae, hexagonally packed cylinders or body centered cubic packing of spheres. We therefore tried to find

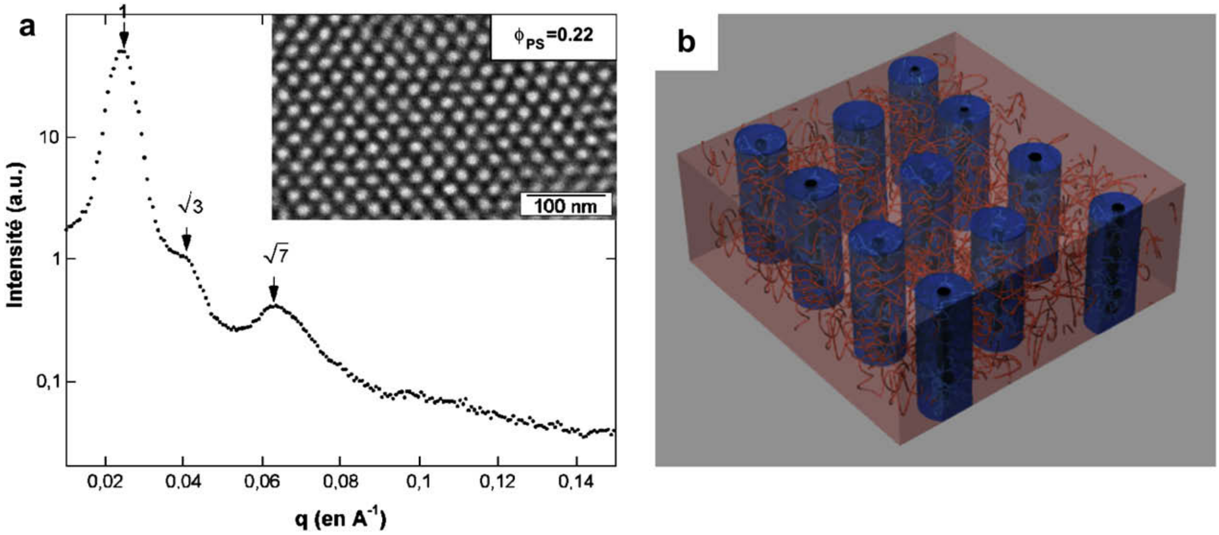

Fig. 4. a) SAXS trace of a bulk sample of ST$_6$-11-34. The inset corresponds to the TEM BF image showing the hexagonal packing of PS cylinders in a PI matrix. b) Schematic illustration of the organization of the block copolymer stars in a PS cylinder morphology. The PI domains are represented in red, PS domains in blue and the C$_{60}$ as black spheres. (For interpretation of the references to color in this figure legend, the reader is referred to the web version of this article.)

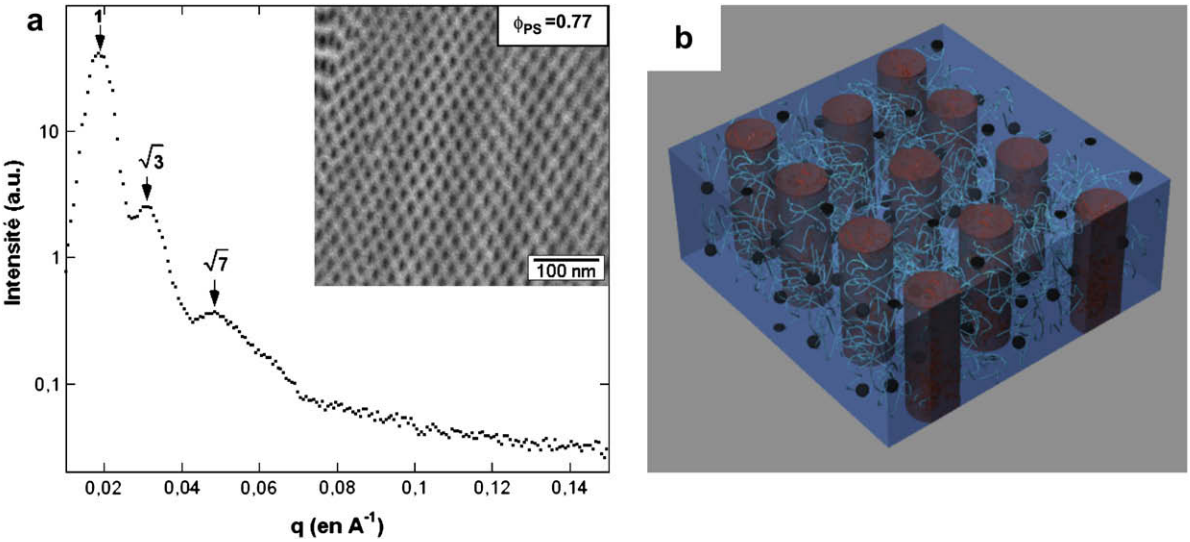

Fig. 5. a) SAXS trace of a bulk sample of ST_6-56-14. The inset corresponds to the TEM BF image showing the hexagonal packing of PI cylinders in a PS matrix. b) Schematic illustration of the organization of the block copolymer stars in a PI cylinder morphology. The PI domains are represented in red, PS domains in blue and the C_{60} as black spheres. (For interpretation of the references to color in this figure legend, the reader is referred to the web version of this article.)

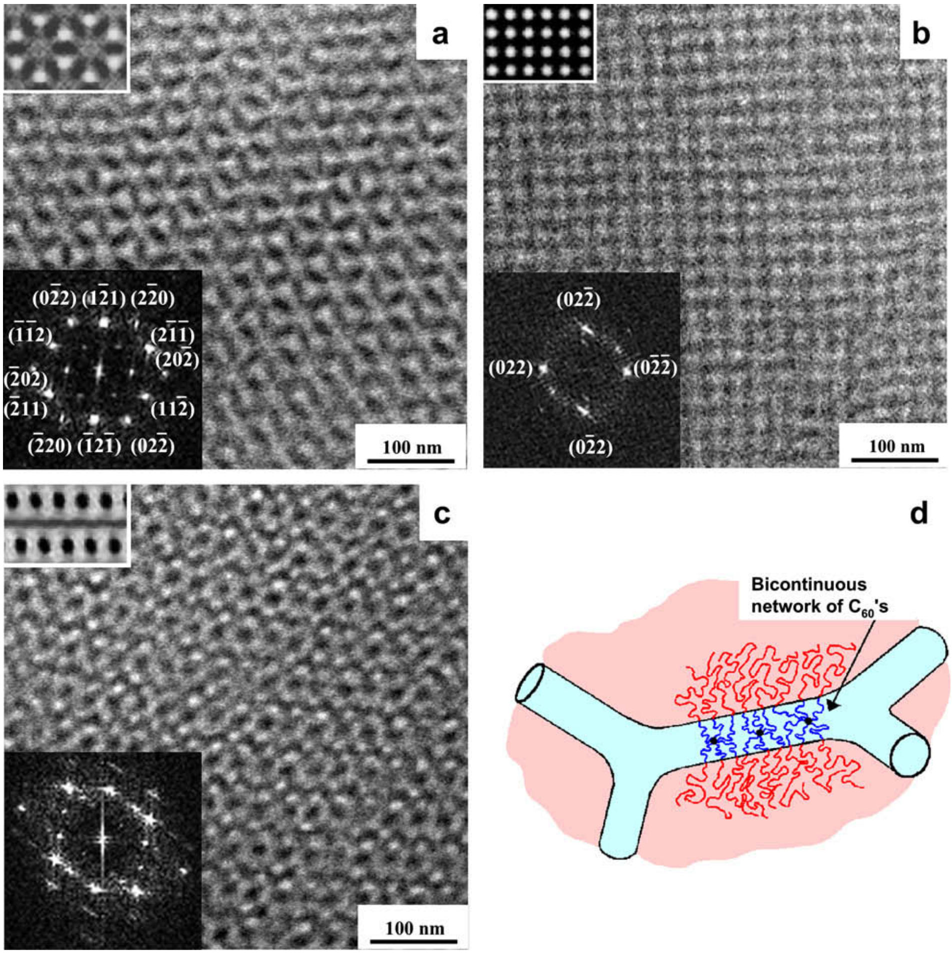

Fig. 6. a–c) Various TEM projections performed on cryo-microtomed sections of ST_6-12-21. 50 nm-thick sections were cut at $T = -80$ °C, coated with an amorphous carbon film and finally stained in vapors of OsO_4 so that PI appears in black. The insets correspond to the FFT (bottom left corners) and simulations (top left corner) using TEMSim software [19]. d) Schematic drawing showing a strut of the PS network of the gyroid structure containing the C_{60}s. (For interpretation of the references to color in this figure legend, the reader is referred to the web version of this article.)

characteristic projections of a cubic structure like the gyroid which can be expected for $f_{PS} = 0.33$ [3]. As demonstrated in Fig. 6, we indeed managed to find such representative patterns characterized by 6-fold (Fig. 6a), 4-fold (Fig. 6b), and 2-fold symmetries (Fig. 6c). The coexistence of these symmetry elements is indicative of a microstructure with cubic symmetry (gyroid, Ordered Bicontinuous Double Diamond). The observed pattern with 6-fold symmetry shown in Fig. 6a corresponds to the most characteristic signature of the gyroid morphology i.e. the so-called “wagon wheel” projection. In addition, it is possible to index the reflections in the corresponding Fast Fourier Transform (FFT) (inset in Fig. 6a) with two sets of {211} and {022} reflections as expected for the gyroid. Note also in Fig. 6a the remarkable resemblance between calculated [19] (inset) and experimental patterns. Another typical projection with 4-fold symmetry is displayed in Fig. 6b. It corresponds to the [100] projection of a gyroid and is furthermore identified by its FFT which shows reflections that can be indexed as {022}. Finally, Fig. 6c presents a third typical pattern which has an apparent 2-fold symmetry and is close to a [110] projection (see calculated [110] projection in the inset of Fig. 6c). All these observations indicate that the microstructure formed by the ST_6-12-21 star is a cubic structure which corresponds most presumably to the bicontinuous gyroid structure.

The observation of a gyroid microstructure for these (PI-*b*-PS)$_6C_{60}$ stars is rather surprising. Indeed, in their study on 18-arm star-block copolymers, Herman et al. proposed that the gyroid structure may be unobtainable unless the minority component is the outer segment of the diblock arm [20]. Clearly, for ST_6-12-21, the outer segment of PI represents the majority phase.

The identification of the microstructure by TEM allows *a posteriori* to index the first diffraction peak observed in the SAXS pattern (See Supporting information S1) as $\sqrt{6}q^*$ and hence to derive the periodicity of the cubic structure of ~56 nm. Earlier reports have predicted that the ratio between the periodicities of the lamellar and the gyroid phases formed by PS-*b*-PI star-block with identical molecular weights should be in the range 2.46–2.14 [21,22]. This ratio, which amounts to 2.33 for ST_6-12-21 and ST_6-25-15, is in very good agreement with earlier observations and theoretical predictions.

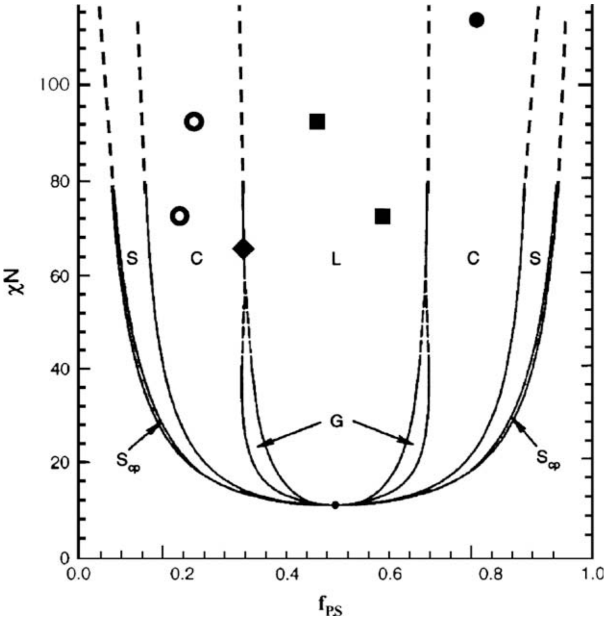

Fig. 7. The different microstructures formed by the self-assembly of (PI-*b*-PS)$_6C_{60}$ stars in the bulk have been plotted on the calculated phase diagram of PS-*b*-PI diblock copolymers [28]. Open and full circles correspond to the cylinder structure (C), full squares to lamellae (L) and the full diamond to the gyroid (G). The dotted lines correspond to the extrapolation of the calculated phase diagram to larger χN values. N corresponds to the number of monomers of the single PS-*b*-PI branch.

Since the core of the stars is a C_{60} molecule, the self-assembly of the PS-*b*-PI copolymer arms allows to build up a periodic and localized nanoscale dispersion of the C_{60} within a bicontinuous 3D network (see Fig. 6d). In addition, the star architecture ensures that the C_{60} cores are preferentially anchored towards the center of the PS channels leading to a reduced inter-fullerene distance despite the low content of C_{60} in the sample. A simple calculation using the molecular weight of the stars and structural considerations relative to the gyroid allows estimating the average distance between successive C_{60}s in the PS channels to ~3 to 4 nm [23–25]. Even if the actual distances between successive C_{60}s may be somewhat larger due to statistical fluctuations of the star's core location in the PS domains, we are able to produce a 3D interconnected network of C_{60}s embedded in an insulating polymer matrix of polyisoprene which should not contain any C_{60}. This controlled confinement allows, even with reduced C_{60} loads (about 0.3 wt%), to achieve continuous paths between C_{60}s. However, even though this original organization of C_{60} in a polymer matrix seems rather interesting in terms of charge transport, this property is presently excluded for two main reasons: i) the inter-C_{60} distance is too large to allow for charge transport by hopping between successive C_{60}s (for efficient charge transport the inter-C_{60} distance should lie below 1 nm) and ii) the reduction of the C_{60} bearing 6 polymer chains is too difficult with respect to the non substituted C_{60} the reported reduction potential for hexa-adducts is −1.87 V vs. ferrocene/ferricinium couple [26,27]. Limitation i) may be overcome by reducing the overall molecular weight of the polymer branches so as to reduce the inter-C_{60} distance. Concerning the second limitation, it could be overcome by the preparation of stars with a reduced number of grafted chains, but this will imply a different synthetic approach for the preparation of star-block copolymers.

4. Conclusion

This study demonstrates that mastering the addition of block copolymers onto a C_{60} molecule to produce well defined star-block copolymers with a C_{60} core opens new and interesting perspectives in terms of spatial organization of fullerenes in a polymer matrix.

All characteristic microstructures reported for PS-*b*-PI diblock copolymers (see Fig. 7) [28] e.g. lamellae, hexagonal packing of cylinders and gyroid were obtained in the case of star-block copolymers (PI-*b*-PS)$_6C_{60}$ by controlling the volume fraction of PS of the stars in the range 0.2–0.77. The strategy presented herein allows to fabricate nanoscale arrays of either “planes” or “threads” of C_{60} in a polymer matrix. Moreover, this study has also clarified certain aspects regarding the structure of 6-arm star-block copolymers. Contrary to earlier reports [20], star-block copolymers with the inner block as the minority phase can indeed organize and self-assemble to form a gyroid microstructure when the number of arms is equal to 6. The present approach may be further developed to prepare materials with interesting electronic properties by: i) decreasing the number of grafted polymer chains on the C_{60} so as to preserve the redox properties of the C_{60} core and ii) reducing the inter-C_{60} distance by lowering the molecular weight of the copolymer arms.

Acknowledgment

We acknowledge gratefully M. Schmutz for stimulating discussions. Technical support by C. Foussat, O. Gavat, A. Rameau and F. Schnell is also acknowledged. S. Lecommandoux, M. Rawiso and J. Combet are acknowledged for performing the SAXS measurements.

Appendix. Supporting information

Supplementary data associated with this article can be found in the online version, at doi:10.1016/j.polymer.2008.12.034.

References

[1] Hamley IW. The physics of block copolymers. Oxford, UK: Oxford Science Publication; 1998.
[2] Lazzari M, Lopez-Quintela MJ. Adv Mater 2003;15:1583.
[3] Fredrickson GH, Bates FS. Annu Rev Mater Sci 1996;26:501.
[4] Lazzari M, Liu GG, Lecommandoux S. Block copolymers in nanoscience. Weinheim, Germany: Wiley-VCH Verlag GmbH & Co., KGaA; 2006.
[5] Tsutsumi K, Funaki Y, Hirokawa Y, Hashimoto T. Langmuir 1999;15:5200.
[6] Bockstaller MR, Lapetnikov Y, Margel S, Thomas EL. J Am Chem Soc 2003;125:5276.
[7] Chiu JJ, Kim BJ, Kramer EJ, Pine DJ. J Am Chem Soc 2005;127:5036.
[8] Ederlé Y, Mathis C. Macromolecules 1997;30:2546.
[9] Mathis C, Schmaltz B, Brinkmann M. C R Chim 2006;9:1075.
[10] Pantazis D, Pispas S, Hadjichristidis N. J Polym Sci Part A Polym Chem 2001;39:2494.
[11] Schmaltz B, Brinkmann M, Mathis C. Macromolecules 2004;37:9056.
[12] Szwarc M. Carbanions, living polymers and electron transfer processes. New York: Wiley-Interscience; 1968.
[13] Audouin F, Nuffer R, Mathis C. J Polym Sci Part A Polym Chem 2004;42:4820.
[14] Pozdnyakov OF, Pozdnyakov AO, Schmaltz B, Mathis C. Polymer 2006;47:1028.
[15] Mathis C, Nunige S, Audouin F, Nuffer R. Synth Met 2001;121:1153.
[16] Picot C, Audouin F, Mathis C. Macromolecules 2007;40:1643.
[17] Ishizu K, Ushida S. Prog Polym Sci 1999;24:1439.
[18] Floudas G, Paraskeva S, Hadjichristidis N, Fytas G, Chu B, Semenov A. J Chem Phys 1997;107:5502.
[19] http://www.msri.org/about/sgp/jim/software/temsim/desc/index.html.
[20] Herman DS, Kinning DJ, Thomas EL, Fetters LJ. Macromolecules 1987;20:2940.
[21] Hadjuk DA, Harper PE, Gruner SM, Honecker CC, Kim G, Thomas EL, et al. Macromolecules 1994;27:4063.
[22] Matsen MW, Schick M. Macromolecules 1994;27:6761.
[23] (a) Thomas EL, Alward DB, Kinning DJ, Martin DC, Handlin DL, Fetters LJ. Macromolecules 1986;19:2127;
(b) Mavroudis A, Avgeropoulos A, Hadjichristidis N, Thomas EL, Lohse DJ. Chem Mater 2003;15:1976.
[24] Gross-Braukmann FJ. Colloid Interface Sci 1997;187:418.
[25] In the gyroid morphology, the length of each strut between two successive nodes is equal to $D\sqrt{2}/4$. Moreover, the length/diameter ratio of a strut at its center is 3:1. If the PS strut is considered as a cylinder, we can deduce the average distance between successive C60s which is given by the following equation:$d_{C_{60}-C_{60}} = M^{*}/N_{\mathrm{A}}\rho_{\mathrm{PS}}(D\sqrt{2}/24)\pi$ where M^{*} is the molar mass of the inner PS core of the star ($M^{*} = 6 \times M_{\mathrm{PS}}^{w}$) in g/mol, ρ_{PS} is the density of PS (we consider that both density of PS and PS star are the same) in g/m^3 and D is the translational period of the unit cell.
[26] Cardullo F, Seiler P, Isaacs L, Nierengarten JF, Haldimann RF, Diederich F, et al. Helv Chim Acta 1997;80:343.
[27] Boudon C, Gisselbrecht JP, Gross M, Isaacs L, Anderson HL, Faust R, et al. Helv Chim Acta 1995;78:1334.
[28] Matsen MW, Schick M. Phys Rev Lett 1994;72:2660.